Argon-like three-electron trajectories in intense-field double and triple ionization

Phay J. Ho and J. H. Eberly

Department of Physics and Astronomy, University of Rochester,
600 Wilson Blvd., Rochester NY 14627, USA.
phayho@pas.rochester.edu

Abstract: We present the double- and triple-ionization momentum distributions obtained from a 3-e planar classical calculation in a laser pulse with peak intensity of 0.8 PW/cm^2. The calculated distributions agree surprisingly well with the experimental Ar^{2+} and Ar^{3+} distributions at the same laser intensity. We demonstrate four recollision pathways that contribute significantly to the production of the doubly and triply charged ions. In particular, the intense-field double ionization pathways are discussed beyond the two-active-electron picture.

OCIS codes: (260.3230) Ionization; (270.6620) Strong-field processes.

References and links

1. D. N. Fittinghoff, P. R. Bolton, B. Chang and K. C. Kulander, "Observation of nonsequential double ionization of helium with optical tunneling," Phys. Rev. Lett. **69**, 2642 (1992).
2. A. Talebpour, C.-Y. Chien, Y. Liang, S. Larochelle and S. L. Chin, "Non-sequential ionization of Xe and Kr in an intense femtosecond Ti:sapphire laser pulse," J. Phys. B **30**, 1721 (1997).
3. S. Larochelle, A. Talebpour and S. L. Chin, "Non-sequential multiple ionization of rare gas atoms in a Ti:Sapphire laser field," J. Phys. B **31**, 1201 (1998).
4. V. L. B. de Jesus, B. Feuerstein, K. Zrost, D. Fischer, A. Rudenko, F. Afaneh, C. D. Schröter, R. Moshammer and J. Ullrich, "Atomic structure dependence of nonsequential double ionization of He, Ne and Ar in strong laser pulses," J. Phys. B **37**, L161 (2004).
5. K. Zrost, A. Rudenko, Th. Ergler, B. Feuerstein, V. L. B. de Jesus, C. D. Schröter, R. Moshammer and J. Ullrich, "Multiple ionization of Ne and Ar by intense 25 fs laser pulses: few-electron dynamics studied with ion momentum spectroscopy," J. Phys. B **39**, S371 (2006).
6. P. B. Corkum, "Plasma perspective on strong field multiphoton ionization," Phys. Rev. Lett. **71**, 1994 (1993).
7. D. G. Lappas, A. Sanpera, J. B. Watson, K. Burnett, P. L. Knight, R. Grobe and J. H. Eberly, "Two-electron effects in ionization and harmonic generation from model He atom," J. Phys. B. **29**, L619 (1996).
8. Phay J. Ho and J. H. Eberly, "In-Plane Theory of Nonsequential Triple Ionization," Phys. Rev. Lett. **97**, 083001 (2006).
9. R. Panfili, J. H. Eberly and S. L. Haan, "Comparing classical and quantum simulations of strong-field double-ionization," Opt. Express **8**, 431 (2001).

Experiments on all inert gas atoms have shown that e-e correlation is essential in leading to the production of doubly charged and higher states in an intense laser pulse over a large range of intensities [1, 2, 3]. With the exception of helium, all the noble gas atoms have 10 or more electrons available to participate even in the double ionization process. These many-electron processes are also known as non-sequential multiple ionization (NSMI). The momentum data suggests that the mechanisms of these NSMI processes are species and intensity dependent [4, 5]. One interesting feature is the origin of the low and high momentum ions present in argon double, triple and quadruple ionization [5]. It is unclear whether both these low and high

#77647 - $15.00 USD Received 30 November 2006; revised 12 February 2007; accepted 12 February 2007

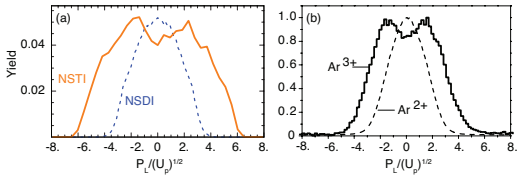

Fig. 1. (a) The sum longitudinal momentum distributions of the doubly ionized (DI) and triply ionized (TI) electrons. (b) The experimental Ar^{2+} and Ar^{3+} longitudinal momentum distributions [5]. Both (a) and (b) are from a 780nm laser pulse with I=0.8 PW/cm^2.

momentum ions can be accounted for by a recollision picture: whether an ionized electron can return to its parent ion with sufficient energy to ionize one or more bound electrons.

Theoretical investigation of the role of recollision (first suggested for double ionization by Corkum [6]) using the time-dependent Schrödinger equation that includes all electrons in argon is currently impossible. A reasonable simplification is to use a few-active-electron model instead. Previous studies have shown the significant improvement achieved with few-electron compared with single electron models (e.g., see [7]). Here, we show that a purely classical model with three active electrons can provide some insights into both double-ionization and triple-ionization momentum distributions of argon.

In this model, the Hamiltonian of a 3-e atom in an intense laser field, $\vec{E}(t)$, is given by

$$\begin{aligned} H &= \sum_{i=1}^{3}\left(\frac{|\vec{p}_i|^2}{2}+\frac{-3}{\sqrt{|\vec{r}_i|^2+a^2}}+\vec{r}_i\cdot\vec{E}(t)\right) \\ &+\frac{1}{\sqrt{(\vec{r}_1-\vec{r}_2)^2+b^2}}+\frac{1}{\sqrt{(\vec{r}_1-\vec{r}_3)^2+b^2}}+\frac{1}{\sqrt{(\vec{r}_2-\vec{r}_3)^2+b^2}}, \end{aligned} \tag{1}$$

with $a=1.0$ and $b=0.25$. In addition to the mechanism of NSTI, this Hamiltonian also gives a minimum basis for investigating the mechanism of multi-electron NSDI, i.e. double ionization beyond the context of two active electrons, as it allows the tracking of three electron pairs throughout the laser pulse. We have previously adopted this Hamiltonian for a generic and classical 3-e model with each electron restricted to move on a 2-d plane that contains the polarization axis and one transverse axis to reproduce the features of experimental NSDI and NSTI ion-count data successfully [8]. In this paper, we calculate the classical NSDI and NSTI electron momentum distributions and examine the pathways of NSDI and NSTI at I=0.8 PW/cm^2.

Surprisingly, even with 3 electrons, this simplified classical model can reproduce both the experimental Ar^{2+} and Ar^{3+} momentum distributions at the same laser intensity extremely well. Figure 1 shows that the width and shape of the calculated momentum distributions along the laser polarization axis (i.e. the longitudinal component) match very well with those obtained from the experiment at the same laser intensity. Notice that both NSDI distributions have a single-peak structure centered at zero, and their cutoffs are at $\pm 4\sqrt{U_p}$, where $U_p = I/(4\omega^2)$ =1.68 a.u. is the ponderomotive energy of an electron at laser frequency, ω=0.0584 a.u. The NSTI distributions, on the other hand, are different from the NSDI distributions. They have a much more complicated structure and are broader than the NSDI distributions. The widths of both the calculated and experimental NSTI distributions extend from -6$\sqrt{U_p}$ to +6$\sqrt{U_p}$, and they have a shallow dip near zero and two side peaks near $\pm 2\sqrt{U_p}$.

These calculated NSDI and NSTI distributions are obtained from the familiar classical ensemble method [9] extended to a 3-e atom. Our atom is represented by a micro-canonical ensemble of 3 million 3-e trajectories in 12-dimensional phase space. With our choice of a and b in eq. (1), these trajectories with initial energy of -4.63 a.u. and zero total angular momentum

#77647 - $15.00 USD Received 30 November 2006; revised 12 February 2007; accepted 12 February 2007

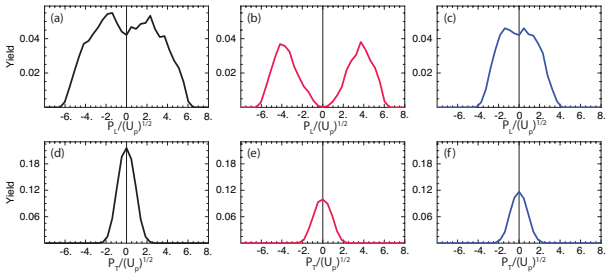

Fig. 2. Top row shows the sum longitudinal momentum distributions of (a) all, (b) NZ and (c) Z triply ionized trajectories. Bottom row shows the sum transverse momentum distributions of (d) all, (e) NZ and (f) Z triply ionized trajectories.

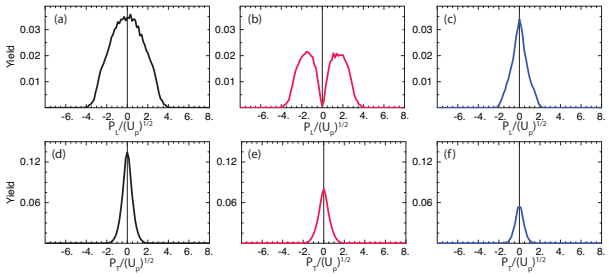

Fig. 3. Top row shows the sum longitudinal momentum distributions of (a) all, (b) NZ and (c) Z doubly ionized trajectories. Bottom row shows the sum transverse momentum distributions of (d) all, (e) NZ and (f) Z doubly ionized trajectories.

are free from auto-ionization and have ionization potential energies of 0.23 a.u., 1.40 a.u and 3.00 a.u. for their singly, doubly and triply ionized charged states respectively.

Each trajectory is subjected to an 780nm ($\omega = 0.0584$ a.u.) laser pulse, that has a longitudinal time-modulated field strength, $E_0 f(t) sin(\omega t + \phi)$, where E_0 is the peak field amplitude, $f(t)$ is the trapezoidal pulse envelope with a symmetric 2-cycle turn-on and turn-off and a 4-cycle plateau, and ϕ is the random carrier envelope phase. We follow the dynamics of the trajectory throughout the laser pulse and determine how many electrons have been ionized and their momenta at the end of the laser pulse. An electron is considered ionized if its kinetic energy is greater than its potential energy. About 16% and 0.4% of the trajectories are found to be doubly and triply ionized respectively. However, the yields of these trajectories and their momentum distributions depend strongly on the pulse shape, and the result will be presented elsewhere.

We start our classical analysis by examining the end-of-pulse positions of three electrons of each NSTI trajectory. Along the laser polarization axis, we found that about half of the NSTI trajectories have all three electrons emitted to the same side of the nucleus, and the remaining trajectories have their electrons located on opposite sides of the nuclear center. These two groups of trajectories predict similar transverse sum momentum distributions, but two different longitudinal sum momentum distributions, as shown in Fig. 2. The same-side-emission trajectories each have a relatively non-zero (NZ) longitudinal sum momentum, and give a well-resolved double-peak distribution with the peaks located at $\pm 4\sqrt{U_p}$, whereas the opposite-side-emission trajectories each have a relatively small or zero (Z) longitudinal sum momentum, and give a rather flat distribution centered at zero.

Similar NZ and Z group can be identified in the NSDI trajectories. However, among the NSDI trajectories, the NZ trajectories are about 1.7 times more likely to occur than the Z trajectories.

#77647 - $15.00 USD Received 30 November 2006; revised 12 February 2007; accepted 12 February 2007

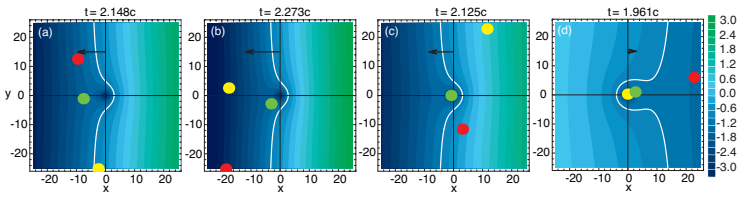

Fig. 4. Animations of the time development of position of three electrons (red, yellow and green balls) in a time-varying combined nuclear and laser dipole potential, leading to the NZ and Z pathways in NSTI and NSDI. Panel (a) shows that the three electrons of a NZ trajectory of NSTI have moved away from the nucleus (the origin) after a recollision (1.6 MB). Panel (b) shows that the green electron of a Z trajectory in NSTI remains trapped near the nucleus while its yellow and red electrons have drifted more than 20 a.u. from the nucleus after a recollision (1.9 MB). Panel (c) shows that the two NSDI electrons (red and yellow) of the NZ pathway have away from the nucleus at t=2.125c (2.1 MB). Panel (d) shows that the red electron of a NSDI Z pathway moves away from the nucleus after recollision while leaving its yellow and green electrons behind (1.7 MB). The x- and y-axis are the laser polarization axis and the transverse axis respectively. The plane is painted with a series of contours with different color shadings that indicate the combined nuclear and laser dipole energies of the electrons, and it is tipped back and forth every half laser cycle. In particular, the elevated and lowered sides have green and blue shadings respectively. For reference, the contour line with a value of -0.6 a.u. is highlighted with a white line. A horizontal arrow is inserted to show the direction and the strength of the time-varying laser force. The timing of the laser pulse is labelleb on top of the movie frame.

Like those NSTI distributions in Fig. 2, both NZ and Z have similar transverse sum momentum distributions, but two different longitudinal sum momentum distributions, as shown in Fig. 3. The longitudinal momentum distribution of NZ and Z trajectories show a double-peak structure with the peaks located near $\pm 2\sqrt{U_p}$ and a narrow distribution centered at zero respectively.

Detailed examination of the histories of all the NSTI and NSDI trajectories throughout the laser pulse reveals that the NZ and Z emission pathways in NSTI and NSDI are initiated by a multi-electron recollision mechanism. Here, we demonstrate the four simplest pathways that produce NZ and Z end-of-pulse trajectories in NSTI and NSDI in four movies. In particular, the recolliding electrons in these pathways move mainly along the laser polarization axis with negligible transverse motion and undergo only one recollision. The pathways with significant transverse recollision motion have been discussed in [8], and the pathways with multiple recollisions will be presented elsewhere.

These four movies in Fig. 4 offer a microscopic view of the NSTI and NSDI process by tracing the individual particle dynamics of three electrons throughout these processes in a 2-d position space and connecting these dynamics with a synchronized laser-modulated nuclear binding potential. In particular, they display the common recollision sequence shared by the NZ and Z trajectories and their differences in the 3-e and 2-e emission sequence. We will first examine the NSTI pathways.

Both NSTI movies start with all three electrons residing near the nucleus. When the field is turned on, these electrons continuously bump into each other and drift around the vicinity of the nucleus under the simultaneous influence of the field and nucleus. The nuclear barrier is periodically elevated or lowered by the laser field. However, such modulation, which is evident from the deformation of the contours, is not strong enough to allow any electron to escape during the first laser cycle. As the laser field continues to grow and reaches a maximum field strength at t=1.250c, the red electron begins to drift away from the core, staying close to the

#77647 - $15.00 USD Received 30 November 2006; revised 12 February 2007; accepted 12 February 2007

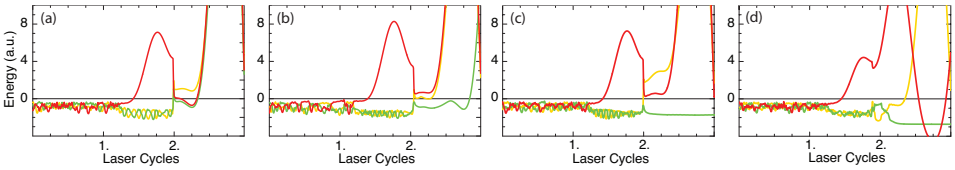

Fig. 5. Time modulation of electron energies, showing the different stages of NSTI and NSDI processes. Panel (a), (b), (c) and (d) record the histories of the NSTI NZ, NSTI Z, NSDI NZ and NSDI Z trajectories of Fig. 4 respectively. In each panel, the red, yellow and green energy lines track the interactions experienced by its red, yellow and green electrons respectively. Here, the energy of each electron is the sum of its kinetic, nuclear, e-e repulsion and laser dipole energy. The random, rapid and negative-energy fluctuations prior to recollision are due to the e-e interaction of one or more bound electron pairs. The relatively slow and smooth energy variation is the signature of dominant laser dipole interaction.

polarization axis, and it eventually disappears from the frame. While the red electron undergoes longitudinal excursion and disappears, the field is not strong enough to ionize the remaining yellow and green electrons. About 1/2 cycle later, the red electron appears from the left side of the frame and approaches the nucleus along the longitudinal axis. It enters the vicinity of the nucleus and collides with the yellow and green electrons when the laser field is close to zero.

The simple recollision scenario described above produces the NZ and Z trajectories for NSTI by having the individual electrons escape the nucleus at different times. In the NZ trajectory, the three electrons rapidly expand away from each other immediately after recollision, and within 0.125c (about 300 attoseconds) the distances between two electrons of 3 individual pairs are already more than 10 a.u. These electrons then promptly leave the nucleus together to the left side. On the other hand, there is a significant time delay between the timing of electron emission and recollision in the Z trajectory. In this case, only the red and yellow electrons move away from the nucleus and disappear from the left side of the movie frame in the same half laser cycle that the recollision takes place. The green electron, however, continues to navigate near the nucleus and does not drift away until the next half laser cycle. Thus, these electron emissions that take places at two consecutive half-laser cycles give opposite-side emission.

These movies alone do not provide information about the e-e interactions, which are the keys that lead to the triple electron ejection in NZ and Z trajectories. Such information, however, can be obtained by examining the time evolution of the electron energies, as shown in Fig. 5 (a) and (b). These plots only display the characteristics of NSTI from t=0 until triple-electron ejection, leaving out the electron's jitter motion due to laser-dipole interaction.

Following the time-modulated energy lines, one can identify two types of e-e interaction, rapid and chaotic collisions between bound electrons and recollision between the ionized and bound electron, that complete the triple-electron emission. In particular, the rapid and chaotic collisions initiate the recollision process in both the NZ and Z trajectories. These collisions prompt quick redistribution of their total energy, which is more or less just their initial 3-e energy, to individual electrons, such that one electron can capture a large fraction of the total energy and maintain this fraction before the next collision. This rapid energy fluctuation coupled with the periodic raising and lowering of the nuclear barrier due to the laser field creates ashort window of time for the red electron in both trajectories to escape the nucleus by having energy higher than the suppressed barrier.

Recollision, on the other hand, is the gateway to triple ionization as it can efficiently channel the field energy into the atomic system. One and more recollisions maybe needed before triple-electron emission depending on the energy transferred to the system. Figures. 5 (a) and (b) show that our NSTI NZ and Z trajectories only require one recollision because large amount of

#77647 - $15.00 USD Received 30 November 2006; revised 12 February 2007; accepted 12 February 2007

energy has been delivered to the system in one recollision.

The amount of energy transferred to the bound electrons combined with the degree of e-e interaction during the recollision give rise to NSTI NZ and Z gateways. In the case of NZ, the recolliding electron has an energy drop of more than 4 a.u. Notice that this energy drop is more than the combined energy of 70 laser photons and, hence, can sufficiently facilitate many highly non-linear processes including NSTI. Interestingly, this step-like energy drop excites both electrons substantially within a time duration of about 20 attoseconds (less than 1/128th cycle, the time step used in the simulation). Consequently, the three electrons interact together very efficiently and extremely briefly before exiting the nucleus.

On the other hand, the Z recolliding electron transfers less than 3 a.u. of energy during recollision. This energy does not excite both bound electrons equally. Notice that the recolliding electron boosts the energy of the yellow electron above the barrier, whereas it only excites the green electron slightly. Subsequently, the red and the yellow electrons leave the core together. The green electron, however, stays in an excited orbit for more than half a laser cycle before exiting the nucleus.

From this triple-ionization Z trajectory, one can deduce that if an even lesser amount of energy is transferred to the green electron such that it will remain bound near the nucleus throughout the laser pulse, the resulting trajectory will then be transformed into a NZ trajectory in NSDI. The corresponding electron energy lines in Fig. 5 (c) show that the energetic recolliding electron provides little or no excitation to the green electron while interacting strongly with the yellow electron. Hence, despite having a third active electron, one can say that this recollision process is effectively a 2-e process and reinforces Corkum's recollision picture of NSDI [6].

The recollision dynamics in the Z pathway for NSDI is rather different from that of the three previous pathways. As shown in the movie, the red recolliding electron returns relatively early near t=1.875c and is deflected in the forward direction after recollision rather than in the backward direction. The result of this recollision is that both bound electrons remain close to the nucleus before the yellow electron escapes near the maximum field strength in the next half laser cycle. The electron energy lines of this pathway, as in Fig. 5 (d), show that even though the recolliding electron carries close to 4 a.u. of energy, it transfers only a very small fraction of its energy to the bound electrons during recollision. This energy leads to immediate and small excitation in both bound electrons. Before the yellow electron can escape, it needs to acquire additional energy from the green electron. Even though the recollision is relatively inefficient, it is still important. Without this recollision, the yellow electron won't be able to escape by merely capturing energy from the green electron. Hence, this pathway includes detailed 3-e excitation and ionization dynamics not present in the existing 2-e NSDI models [4, 6].

In summary, a large ensemble of 3-e classical trajectories produces argon-like double- and triple-ionization momentum distributions at I=0.8PW/cm^2. Our classical analysis suggests that, in both the NSDI and NSTI processes, the high and low momentum Ar ions mainly come from the NZ and Z trajectories, i.e. trajectories have and do not have all ionized electrons ejected to the same side along the laser polarization axis, respectively. A multi-electron recollision can initiate these different NZ and Z trajectories of NSTI and NSDI, depending on the degree of e-e interaction and energy of the recolliding electron. If substantial e-e interactions among the 3 electron pairs can be initiated, the three electrons can then acquire enough energy and, subsequently, escape the nucleus either together in an attosecond timescale or at different half laser cycles. On the contrary, if the recollision does not create a substantial 3-e interaction, then 2-electron emission is more likely to take place.

Acknowledgement: This work was supported by DOE Grant DE-FG02-05ER15713. We appreciate several conversations with Prof. S. L. Haan from Calvin College.

#77647 - $15.00 USD Received 30 November 2006; revised 12 February 2007; accepted 12 February 2007